THE AMERICAN SOCIETY OF MECHANICAL ENGINEERS
345 E. 47th St., New York, N.Y. 10017

97-GT-496

Effects of Stator Indexing on Performance in a Low Speed Multistage Axial Compressor

Wendy S. Barankiewicz
National Aeronautics and Space Administration
Lewis Research Center
Cleveland, Ohio

Michael D. Hathaway
Vehicle Technology Center
U. S. Army Research Laboratory
Cleveland, Ohio

ABSTRACT

The results of an experimental investigation to determine the impact of stator row indexing or clocking on multistage axial compressor performance are presented. Testing was conducted in the NASA Lewis Research Center's Four-Stage Axial Compressor Facility. The impact of stator row indexing on both the overall and stator 3 blade element performance is presented for both the peak efficiency and peak pressure operating conditions. The change in overall performance due to stator indexing is 0.2% for both operating conditions. Indexing resulted in a 5% change in stator 3 mass averaged loss coefficient at the peak efficiency condition and a 10% change at the peak pressure condition. Since the mass-averaged stator 3 loss coefficient is on the order of 7%, the changes in loss coefficient due to indexing are on the order of 0.35-0.7%. These changes are considered to be small and are of the same order of magnitude as the passage-to-passage differences in loss coefficient due to manufacturing and assembly tolerances in the test compressor. The effects of stator-stator wake interactions are also shown and indicate that for rows with unequal blade counts it may be necessary to survey across more than one blade row pitch for accurate blade row performance measurements.

NOMENCLATURE

A	Annulus area, m^2
C_d	Bellmouth discharge coefficient
C_{p_s}	Static pressure coefficient = $(P - P_{ref})/(\frac{1}{2}\rho_{ref}U_{tip}^2)$
C_{p_t}	Total pressure coefficient = $(P^o - P_{ref})/(\frac{1}{2}\rho_{ref}U_{tip}^2)$
ΔH_{isen}	Isentropic head rise per stage = $\frac{1}{4}\frac{\gamma}{\gamma-1}\frac{P_{ref}}{\rho_{ref}}\left[\left(\frac{P_{out}}{P_{in}}\right)^{\frac{\gamma}{\gamma-1}} - 1\right]$
$\dot{m}$	Mass flow rate = $C_d\dot{m}_{1d}$, kg/sec
$\dot{m}_{1d}$	Theoretical one-dimensional massflow rate, kg/sec
N	Stage number
P	Pressure, Pa
U_{tip}	Rotor blade tip speed, m/sec
ϕ	Flow coefficient = $\dot{m}/(\rho_{ref}AU_{tip})$
Γ	Shaft torque, Nm
η	Efficiency = $\Psi/[\Omega(\Gamma - \Gamma_{tare})/(\frac{1}{2}\dot{m}U_{tip}^2)]$
$\Delta\eta_{est}$	Estimated efficiency change
ρ	Density, kg/m^3
ω	Total pressure loss coefficient = $(P_1^o - P_2^o)/(P_1^o - P_1)$
Ω	Rotor speed, radians/sec
Ψ	Static pressure rise coefficient per stage = $\Delta H_{isen}/(\frac{1}{2}\rho_{ref}U_{tip}^2)$
Δ	Maximum difference for all indexing configurations

Subscripts

1	Stator row inlet station
2	Stator row exit station
in	Compressor inlet station, upstream of first rotor
out	Compressor outlet station, downstream of last Stator
ref	Reference conditions measured in plenum
mean	Arithmetic average over all indexing configurations
avg	Arithmetic average of repeated trials

Superscripts

o	Total conditions
—	Mass averaged

INTRODUCTION

With turbomachinery designers continually challenged to achieve greater pressure rise in fewer stages while maintaining or increasing

Presented at the International Gas Turbine & Aeroengine Congress & Exhibition
Orlando, Florida — June 2–June 5, 1997

efficiency, the need for better understanding of fundamental multistage flow physics and greater modeling fidelity increases. One such aspect of turbomachinery design that comes up from time-to-time is whether there is any potential for significantly improving multistage performance by accounting for the relative circumferential position (indexing) of adjacent stator (or rotor) rows. The concern is what effect the impingement of upstream stator/rotor wakes have on the performance of downstream stators/rotors. Previous research consists primarily of investigations of indexing effects in turbines with a few investigations for compressors focusing on the impact of stator indexing on noise production.

Arndt (1991) used both surface mounted hot film and hot-film probe measurements in a five stage moderately high-aspect-ratio low-pressure turbine to study the unsteady flow phenomena due to rotor-rotor and stator-rotor wake interactions. Both rotor-rotor and stator-rotor interactions were observed to have a profound and approximately equal influence on the flow through the turbine. Interaction of rotors of different stages occurred due to the influence of wakes shed by one rotor row impacting the flow through the following rotor row. This wake induced rotor-rotor interaction resulted in strongly amplitude-modulated periodic and turbulent velocity fluctuations downstream of every rotor row with the exception of the first rotor.

In a two part paper, both experimental (Huber, et al 1995) and analytical (Griffin, et al 1995) studies were conducted to investigate the impact of stator indexing on the performance of the Space Shuttle Main Engine Alternate Fuel Turbopump Turbine test article. This is a two and one half stage turbine which was modified to provide equal stator blade count between stages. These studies concluded that there was a measurable difference in efficiency ($\sim$ 0.3%) for both high and low Reynold's number flows due to stator indexing effects. Based on three dimensional time accurate Euler calculations and two-dimensional time accurate Navier Stokes analyses, the measured maximum efficiency occurred when the calculated time average first vane wake impinged upon the second vane leading edge. Conversely, the minimum efficiency occurred when the first vane wake was calculated to be in the second vane mid-channel. The Navier Stokes simulations indicated that improved performance of the second vane is a major contributor to the turbine efficiency benefits achieved through stator indexing. Reduced surface velocities and less large-scale unsteadiness on the second vane were noted as possible reasons for the improved second vane performance. Based on measured spanwise variations in local efficiency, the study concluded that if the first vane wakes could be properly aligned with the second vane leading edge from hub to tip, a 0.8 percentage point improvement in turbine performance would be possible.

Engel, et al 1995 used a time-accurate two-dimensional Navier-Stokes solver to investigate stator indexing effects in a stator-rotor-stator turbine configuration. They analyzed the stator-rotor-stator combination for two stator indexing configurations: 1) with stator 2 aligned with stator 1, and 2) with stator 2 one-half stator pitch offset from stator 1. They concluded from their analysis that the overall losses in the exit of the second stator differed by 2-4% for the two index configurations, and that a substantial part of the loss production was due to unsteady phenomena.

Reported investigations of stator indexing in multistage axial compressors have primarily focussed on compressor noise. Walker (1972) and Walker and Oliver (1972) measured a considerable noise reduction (5-6 db) from a one and one half stage axial compressor when circumferential relative stator positions where properly chosen. They concluded that the interaction of wakes between successive blade rows can be used to reduce the velocity deficiency within those wakes and so reduce the amount of noise produced. The impact of stator indexing on sound pressure level has also been confirmed by Schmidt and Okiishi (1977). They further reported that no measurable difference in hydraulic efficiency could be detected between the minimum and maximum noise conditions. To the authors' knowledge, there has been no other published research reporting the impact of stator indexing on multistage compressor performance.

The purpose of this investigation is to quantify the effect that circumferential indexing of stator rows relative to one another has on overall and blade element performance. The NASA four-stage Low-Speed Axial Compressor (LSAC) was used as the test article for this investigation. The LSAC has four geometrically identical stages, and as such provides the greatest potential for measuring the performance impact of stator indexing. When consecutive stator blade rows contain the same number of blades per row, the stator rows can be circumferentially located in such a way that the wakes from each upstream blade will impinge on the adjacent downstream stator blade row leading edges. Since most multistage compressors have a different number of stator blades in each stage, with the exception of some aft stage sets, the potential for performance gains due to stator indexing is expected to be even less than that measured in the present effort.

A "baseline" index configuration in which all stator wakes impinge on the adjacent downstream stator leading edges was first established. Overall performance measurements were then acquired as a function of stator row indexing to define the minimum and maximum indexing effect at peak efficiency and peak pressure conditions. Detailed area surveys were then conducted both upstream and downstream of the third stage stator row for selected indexing configurations to investigate the impact of indexing on stator loss.

TEST COMPRESSOR AND INSTRUMENTATION

Test Compressor

The NASA Lewis Research Center's Low-Speed Axial Compressor consists of an inlet guide vane and four geometrically identical stages designed for accurate low-speed simulation of a high-speed multistage core compressor. The blades were aerodynamically scaled and modeled after General Electric's Energy Efficient Engine blading (Wisler, 1977). Figure 1 shows an illustration of the NASA Low Speed Axial Compressor, and Table 1 contains the pertinent design parameters of the LSAC. Additional information can be found in Wasserbauer, et al 1995.

The design philosophy of the LSAC closely follows that of the GE Low-Speed Research Compressor. A long entrance length (not shown in Figure 1) develops thick endwall boundary layers typical of an embedded stage, while the first two stages set up the multistage environment. The third stage is the test stage, and the fourth stage acts as a buffer to the exit conditions. The stators are designed with end bends at both the hub and the case which result in the blade leading edge, trailing edge, and blade setting angles changing approximately 10 to 16 degrees over the inner and outer 30% of blade span from the endwalls (Wellborn, 1996).

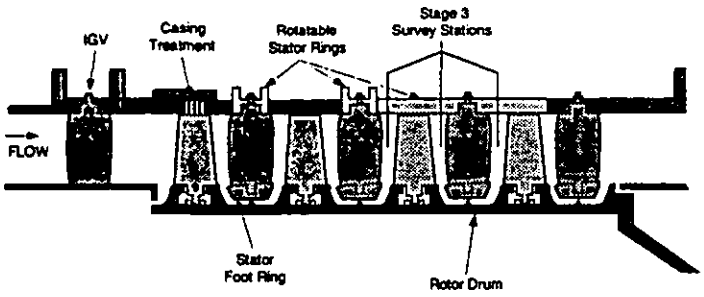

Figure 1 Schematic of NASA Low Speed Axial Compressor.

Figure 1 NASA Lewis Low Speed Axial Flow Compressor.

Table 1 Design Parameters for the Low Speed Axial Compressor

Rotor blade tip speed	61.0 m/s
Rotative speed	980 rpm
Axial velocity	24.4 m/s
Mass flow	12.3 kg/s
Pressure ratio	1.042
Temperature ratio	1.013
Tip radius	61.0 cm
Hub radius	48.8 cm
Aspect ratio (span/chord)	
Rotor	1.20
Stator	1.31
Axial chord at midspan	
Rotor	7.6 cm
Stator	6.6 cm
Blade setting angle at midspan	
Rotor	43°
Stator	42°
Number of Blade	
Rotor	39
Stator	52
Axial blade row gap at midspan	2.54 cm
Clearance	
Rotor tip	1.40 % span: 0.17 cm
Stator seal	0.78 % span: 0.09 cm

The LSAC has the capability of independently rotating the first three stator blade rows approximately two stator pitches via remote controlled actuators. Thus, the relative circumferential position of the first three stator rows and either the IGV or fourth stator row can be varied (i.e., stator indexing). This is accomplished by mounting each of the first three stator rows in circumferential rings (see Figure 1) which are trapped in roller cages attached to the casing. The IGV and fourth stage stator rows are fixed. After an indexing configuration is established by rotating stator rows relative to one another, probe area traverses are accomplished by moving the first three stator rows in unison (with the indexing configuration "frozen") past stationary probes mounted in radial actuators attached to the casing.

Probe area traverses ahead of and behind the fixed IGV and fourth stage stator rows are accomplished by traversing probes which penetrate through circumferential slots in the casing. These probes are mounted in radial/circumferential actuators fixed to the casing.

Instrumentation

Overall performance measurements were based on casing static pressures (for overall pressure rise coefficient) and bellmouth massflow (for flow coefficient). The overall pressure rise coefficient, expressed on a per stage basis, was calculated based on the arithmetic average of the inlet and outlet static pressures. For the pressure rise coefficient calculation it was assumed that the rise in static pressure equaled the rise in total pressure. The inlet station is located 1.25 rotor chords ahead of the first rotor (0.85 IGV chords behind the IGV), and the outlet station is located 1.43 stator chords behind the last stator. Each station contained four outer wall (casing) static pressure taps circumferentially located midway between the stator blades at 90° intervals. The flow coefficient was calculated based on the theoretical one-dimensional massflow rate and a previously determined Reynolds-number-dependent discharge coefficient. The theoretical massflow rate was determined from compressible flow relations assuming isentropic flow from the bellmouth and constant static pressure at the massflow measurement station. Stagnation properties were obtained from reference conditions measured in the plenum, while the static pressure was obtained from the average of casing and hub static pressure measurements at the massflow measurement station. The massflow measurement station was located downstream of the bellmouth throat and far upstream of the compressor inlet. The pressures used in the massflow calculation were measured with 1.8 Pa (0.0003 psi) resolution pressure transducers which were kept in an environmentally controlled chamber to minimize transducer zero drift. A humidity meter mounted near the plenum inlet was used to correct the measured massflow for humidity. Compressor speed was measured from a magnetic speed pickup.

Efficiency (η) was calculated by taking the ratio of the static pressure rise coefficient to the work coefficient. Since this is a low speed machine with negligible temperature rise, the work coefficient was based on the net torque obtained by subtracting the tare torque from the measured torque. The tare torque was obtained by measuring the shaft torque with all blades removed and with a smooth rotor drum (i.e., all rotor and stator ring cavities were closed off), and subtracting off the hub windage drag which was charged to the compressor. The windage drag was estimated based on Schlicting's (1979) correlation to calculate the skin friction coefficient for flat plate turbulent boundary layers at zero pressure gradient. Probe surveys of the hub boundary layer confirmed the turbulent boundary layer profile. Since the compressor is laid out horizontally with the rotor drum overhanging the forward bearing, there are high transverse forces on the journal bearings, resulting in a large tare torque. Furthermore, the tare torque includes not only the torque due to windage drag and bearing friction, but also friction drag due to carbon seals used in a pneumatic slip ring located between the compressor and torque meter. The tare torque changes as the carbon seals wear. Although the measured absolute efficiency

level is not accurate, incremental changes in efficiency are generally reliable if acquired in a short test program during which the wear of the carbon seals can be assumed negligible.

Blade element performance data were acquired based on miniature (1.64 mm) Kiel head probes for measuring total pressure loss and 18-degree wedge probes for measuring static pressure and flow angle. For each measurement station the Kiel probe yaw angles were set once at the beginning of a circumferential probe traverse using the measured average yaw angles from wedge probes located at the same axial and radial measurement location. This method was deemed satisfactory since the yaw angle typically varied less than 10 degrees across the stator pitch, and the uncertainty in the total pressure coefficient measured by the Kiel probes was less than 0.1% over a ±40 degree range of yaw angle as determined from probe calibrations. The Kiel probe yaw angles were adjusted in this manner for each span and indexing configuration.

Stator total pressure loss was obtained by connecting Kiel probes located ahead of and behind the stator blade row at the same radial and circumferential position in the annulus to a 1.8 Pa (0.0003 psi) differential pressure transducer. The upstream total pressure was simultaneously measured using a separate transducer. The uncertainty in total pressure loss coefficient is difficult to assess, but is estimated to be about 2% ($\Delta\omega$ = 0.0015) based on uncertainty analysis of the mid-span survey measurements at peak pressure condition. A complete uncertainty analysis for the LSAC measurement system is provided by Wellborn, 1996.

The circumferential probe traverses acquired at each span started and ended in the freestream region between stator wakes. Thus, the measured distributions of total pressure coefficient were essentially periodic with the measured difference in total pressure coefficient between the start and end of the survey being generally less than 0.3% but no greater than 0.7% of the measured mass averaged total pressure coefficient. In any case, the average of the starting and ending total pressures was used to establish periodicity in calculating the circumferential mass averaged conditions.

Spanwise distributions of stator total pressure loss coefficient were determined from the area surveys as follows: 1) Circumferential mass-averaged conditions were determined at 14 measurement points along the span. 2) The measured spanwise distributions were interpolated to 100 equally spaced points across the span, and then integrated from the casing toward the hub to determine the radii which correspond to 10% mass flow fractions at each axial survey location. 3) The interpolated spanwise distributions of total and static pressures were then mass-averaged across the span of each stream tube determined in step 2 to arrive at an average value for that stream tube. An overall mass averaged stator 3 total pressure loss coefficient for each indexing configuration was calculated by mass averaging the measured spanwise distributions of total and static pressures at each measurement station obtained from step 1 above.

TESTING SETUP/PROCEDURE

The relative stator circumferential positions that would result in upstream stator wakes impinging on adjacent downstream stator leading edges were determined from circumferential surveys of total and static pressure measurements obtained by rotating individual stator rows relative to fixed Kiel and wedge-static probes. Since both the IGV and the fourth stage stators do not rotate, it was not possible to align all five blade rows. We chose to not align the wakes from the IGV's since the IGV's are lightly loaded, are located about one stator chord upstream of the first rotor, and are therefore considered to have minimal impact on the test stage (stator 3).

The procedure described below was performed with the probes located at midspan for two different operating conditions: peak pressure and peak efficiency. Stator leading edge locations were determined first based on static pressure measurements obtained from a stationary auto-nulling wedge probe installed just upstream of a stator row. The stator row was rotated at least one stator pitch while all other stator rows were held fixed. The stator leading edge was taken as the position of maximum static pressure (i.e., at the stator stagnation point) on a plot of static pressure coefficient (Cps) versus stator circumferential position as depicted in Figure 2a.

The relative circumferential position of the upstream stator row which results in its shed wakes impinging on the leading edges of the target stator row were determined from total pressure measurements obtained from a stationary Kiel probe installed in place of the wedge probe with the target stator set to the circumferential position corresponding to maximum Cps as determined in the previous step described above. The upstream stator was then rotated at least one stator pitch to determine the upstream stator position corresponding to minimum total pressure on a plot of total pressure coefficient versus stator circumferential position as depicted in Figure 2b.

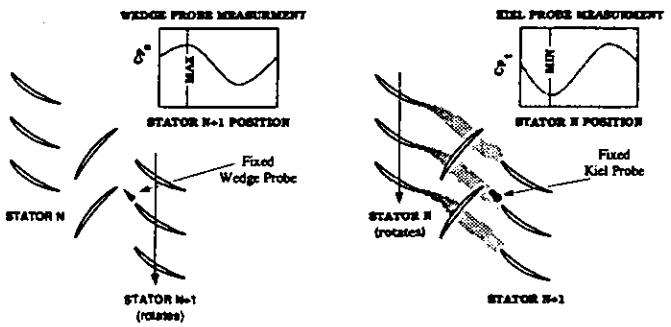

a) Position of Stator N+1 Relative to Probes b) Position of Stator N Wake Relative to Stator N+1

Figure 2 Determination of the Stator Relative Positioning.

The procedure described above was first used to align stator 1 wakes with the stator 2 leading edges. Stator 1 and 2 were then moved in unison and the procedure was repeated to align stator 2 wakes with the stator 3 leading edges. Finally, stators 1, 2, and 3 were moved in unison to align stator 3 wakes with the stator four leading edges. The position of those stators held fixed during the course of the above measurements were determined to have no effect on the determination of the relative stator leading edge or wake circumferential locations. There were slight decreases or increases in the background pressure level outside the wakes depending on the positions of the fixed stator rows relative to the probes, but no effect on the measured circumferential locations of maximum Cps or minimum Cpt.

With the relative stator circumferential positions arranged as described above it was assumed that the wakes from each stator row impinged on the leading edges of the adjacent downstream row. This configuration was considered the baseline indexing configuration (i.e., 0% pitch indexing case). A different baseline indexing configuration

as established for peak efficiency and peak pressure conditions. Other indexing configurations were then arranged by moving all stator rows circumferentially relative to each other in fractions of stator pitch from the appropriate baseline indexing configuration. Figure 3 schematically illustrates the relative stator wake positions for various indexing configurations. Measurements acquired across the span indicated that the maximum Cps and minimum Cpt (i.e., stator leading edge, and wake positions) were relatively independent of span (except very close to the endwalls) as shown in Figure 4.

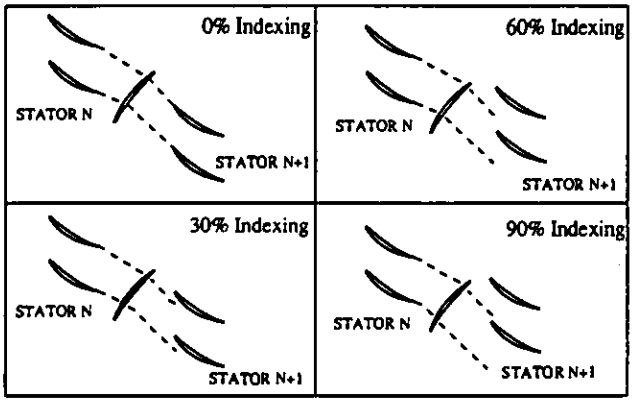

Figure 3 Stator Wake Indexing Alignment (Throughout Compressor).

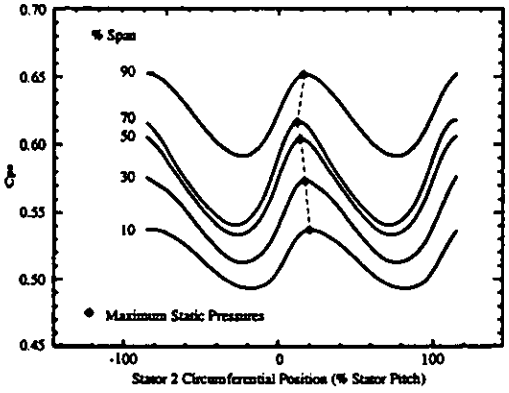

a) Static Pressure Upstream of Stator 3

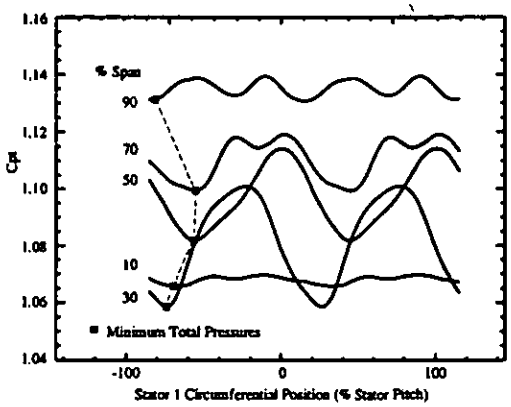

b) Total Pressure Upstream of Stator 3

Figure 4 Spanwise Variation of the Circumferential Distribution of Pressure Coefficient.

The test procedure consisted of two parts: In Part I, the overall compressor performance was measured at two operating conditions (peak efficiency, and peak pressure) as a function of stator indexing. In Part II, several indexing configurations including the "best" and "worst" configurations for each operating condition were investigated further by conducting detailed area traverses upstream and downstream of stator 3 to assess the impact of stator indexing on the stator 3 blade element performance.

The stator 3 probe area traverses were accomplished by positioning all Kiel and wedge static probes upstream and downstream of stator 3 to the same radial locaion and then for a given indexing configuration collectively traversing the first three stator rows circumferentially past the stationary probes. At each radial location circumferential traverses were accomplished for all indexing configurations surveyed. The probes were then successively moved to each radial location until all spanwise surveys were accomplished, thus completing area traverses for all indexing configurations.

RESULTS AND DISCUSSION

The following discussion of results describes not only the impact of stator indexing on overall and stator 3 blade row performance, but also describes how wakes from adjacent blade rows can interact such that the wakes appear to be mixed out.

Overall Performance

Since the effects of the stator indexing configuration were anticipated to be dependent on operating condition, performance data were acquired for two different flow conditions, peak efficiency and peak pressure. These operating points are shown on the overall performance map presented on a per-stage basis for one indexing configuration in Figure 5. Measurements of overall performance were acquired for stator indexing configurations corresponding to every 10% of stator pitch starting from the baseline indexing configuration (where all stator wakes impinge on the adjacent downstream stator leading edges).

To assess measurement uncertainty, the measurements of overall performance as a function of stator indexing configuration were repeated 10 times for both the peak efficiency and peak pressure conditions, Figures 6a and 6b respectively. For each stator indexing configuration, the data were then arithmetically averaged over all 10 trials to obtain distributions of the averaged overall performance as a function of stator indexing configuration.

For the peak pressure case (see Fig. 6a), the overall performance measurements from the 10 trials were very repeatable, with the uncertainty in the average per stage static pressure rise for a given indexing configuration (based on a 95% confidence interval) being on the order of ±0.02 % of the mean per stage static pressure rise. Based on the averaged overall performance, the maximum variation in per stage static pressure rise due to stator indexing was measured to be 0.29 % of the mean per stage static pressure rise. Note that there is a significantly larger variation in overall performance between different stator indexing configurations than between trials, and that the overall shape of the distributions of performance as a function of stator indexing configuration are the same for each trial (i.e., overall performance is clearly stator index configuration dependent).

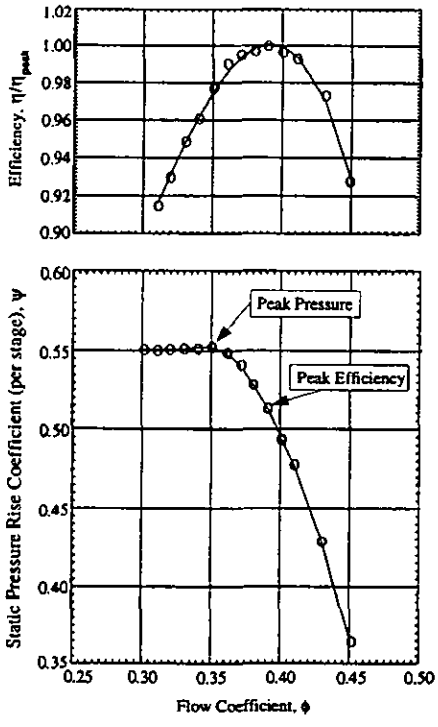

Figure 5 LSAC Performance Map.

For the peak efficiency operating conditions (see Fig. 6b), the overall performance measurements from the 10 trials are much less repeatable than for the peak pressure condition. The uncertainty (based on measurement repeatability) in the average per stage static pressure rise at the peak efficiency operating condition is ±0.10 %, which is five times greater than that of the peak pressure condition. The maximum variation in averaged per stage static pressure rise as a function of stator index configuration for the peak efficiency condition is 0.24 %, which is approximately the same as for the peak pressure condition.

The difference in repeatability for the two operating conditions is predominantly due to the differences in the slopes of the pressure rise characteristic at each operating condition (see Fig. 5). At the peak efficiency condition, a small fluctuation in flow will result in a much larger pressure rise perturbation than at the peak pressure condition.

The distributions of overall performance as a function of stator indexing configuration for the two tested operating conditions are stator-pitch phase shifted (i.e., the stator index configuration that yields the maximum pressure rise for the peak pressure condition yields the minimum pressure rise for the peak efficiency condition). One possible explanation for this difference is that stator indexing affects stator deviation and thus work input which results in the maximum pressure rise occurring at different indexing configurations for peak efficiency and peak pressure conditions. Also, the turbulence of the upstream stator wakes impinging on the downstream stators should be helpful near peak pressure rise in suppressing separations, but deleterious near peak efficiency because it will encourage early transition and thus thicken the boundary layers.

Stator 3 Blade Performance

To assess the stator 3 blade performance, detailed area surveys

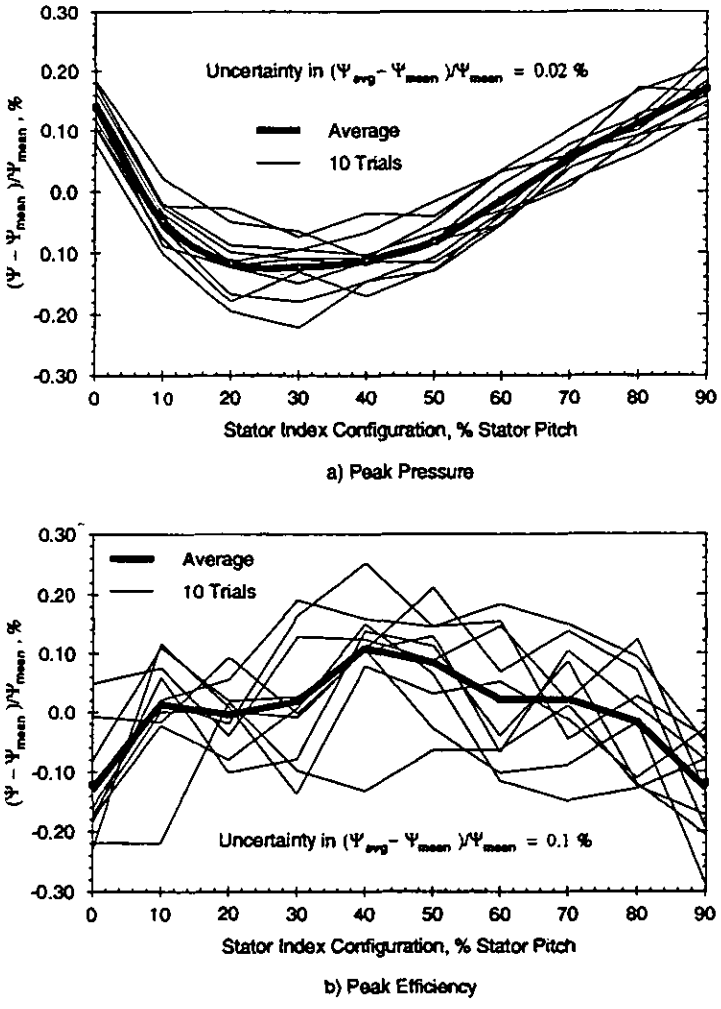

Figure 6 Overall Performance Variation with Stator Indexing.

were acquired across one stator pitch at three axial locations: ahead of rotor 3, ahead of stator 3, and behind stator 3. Surveys were acquired for both peak pressure and peak efficiency conditions at four to five stator indexing configurations, including the maximum and minimum pressure rise configurations as determined from the averaged overall performance data (Fig. 6).

Spanwise distributions of total pressure loss coefficient are plotted in Figures 7a (peak pressure) and 7b (peak efficiency) for the indexing configurations that correspond to the maximum and minimum stator 3 total pressure loss coefficient. A mean total pressure loss coefficient at a particular operating point was determined by arithmetically averaging the stator 3 mass-averaged loss coefficients measured for each indexing configuration. The mean value was then used to calculate the percentage difference in loss coefficient for each indexing configuration. The maximum difference in total pressure loss coefficient due to indexing was 10% for the peak pressure case, and 5% for peak efficiency. For peak pressure the indexing configurations corresponding to minimum/maximum stator 3 loss coefficient were consistent with the stator indexing configurations corresponding to maximum/minimum overall pressure rise coefficient.

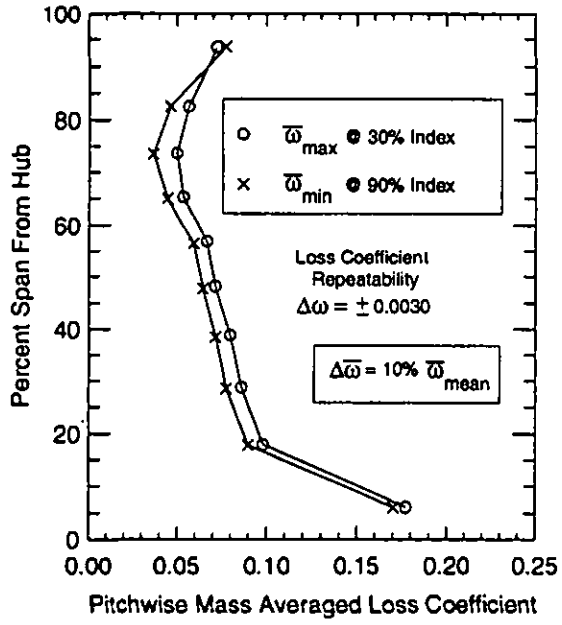

a) Peak Pressure

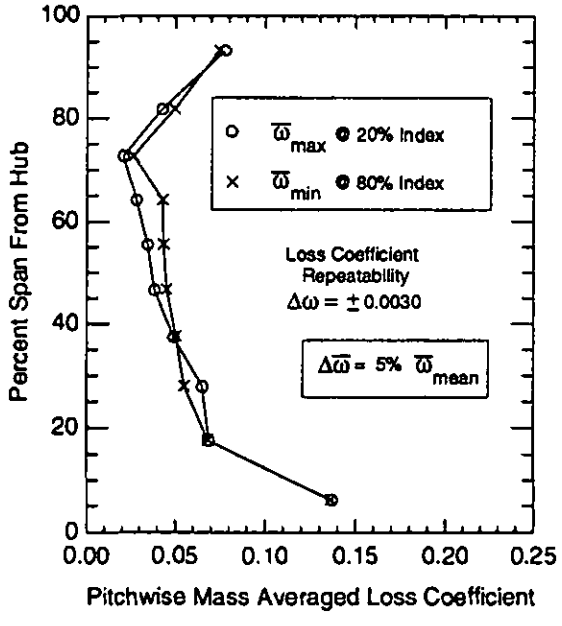

b) Peak Efficiency

Figure 7 Stator 3 Mass Averaged Total Pressure Loss Coefficient Calculated at 10% Stream Tube Increments for Indexing Configurations Corresponding to Minimum and Maximum Loss at Each Operating Condition.

As is evident from Figure 7 the results of the peak pressure condition have a much smoother and more consistent trend of total pressure loss variation than for the peak efficiency condition. In general all data acquired at the peak pressure condition is "better behaved" than at the peak efficiency condition. At peak efficiency condition the compressor speed line characteristic is steepest ($\Delta\Psi/\Delta\phi = -1.76$), while at the peak pressure condition the slope of the compressor characteristic is nearly zero ($\Delta\Psi/\Delta\phi = -0.08$). Therefore, repeatability (0.41%) and variation (0.14%) in flow coefficient have a larger impact on total pressure rise coefficient at peak efficiency than at peak pressure. Detailed analysis of the circumferential survey data acquired at each span shows differences due to changes in both stator loss and rotor work input as a result of indexing, but provides no clear explanation for the differences in character of the total pressure loss distributions for the two conditions tested.

One possible factor is the nature of the secondary flows in the stator. The stators were designed with end bends at both the hub and casing which significantly change the stator blade leading edge, trailing edge, and blade setting angles over the inner and outer 30% of blade span. All indexing patterns tested were based on mid-span surveys only. At peak pressure the stator wakes are wider and deeper as well as being in a region where the total pressure rise characteristic is flat. Therefore, it is reasonable to expect that the peak efficiency condition may be more susceptible to small spanwise changes along the span due to stator indexing. Furthermore, the stator end bends promote secondary flows which cause spanwise redistribution of flow. The affect of the stator end bends on flow redistribution may also be more significant at peak efficiency where there is essentially no flow separation (based on ammonia/ozalid flow visualization at one indexing configuration) as opposed to peak pressure where there is a significant hub corner separation.

Since the measured variations in loss coefficient due to indexing shown in Figure 7 are two to five times larger that the measurement uncertainty, we are confident that there is indeed a detectable, albeit small stator loss penalty associated with indexing. To provide some perspective on the measured changes in loss coefficient due to indexing, two adjacent blade passages were surveyed at one indexing configuration to document the blade-to-blade loss variations caused by manufacturing and assembly tolerances. For these comparisons the measured difference in total pressure loss coefficient for the two blades was based on the arithmetic average of pitchwise surveys conducted at only 30, 50, and 70% span. The resultant difference in loss coefficient due to manufacturing and assembly differences between the two passages was found to be 7% for peak pressure and 4% for peak efficiency relative to their respective index-mean values. These are of the same order of magnitude as the loss differences due to stator indexing. These estimates are based on measurements of only two adjacent stator passages, and thus are not necessarily representative of the typical or maximum differences due to manufacturing and assembly tolerances. The blade surface contours are within ±0.05 mm (0.002 inches) of design and the blade setting angles were estimated to be within ±0.2 degrees of each other.

A summary of the effects of indexing on the overall and stage 3 performance is presented in Table 2. For reference, the effects due to blade-to-blade variations are also presented. As previously mentioned in the instrumentation section efficiency was difficult to measure accurately. Since the actual tare torque is not known, the estimated changes in overall efficiency provided in Table 2 are based on measured torque with tare torque adjusted to provide a peak efficiency of 0.9. Indexing effects are measurable, changing overall efficiency on an average of 0.2 percentage points.

Note from Table 2 that the effects of blade-to-blade variations are about the same as those due to indexing. Note also that as the compressor becomes more heavily loaded as the flow is reduced from

peak efficiency to peak pressure, the changes associated with both of these loss mechanisms becomes more pronounced, as should be expected since the stator wake deficit increases. As can be seen from Table 2 at the peak pressure condition, the changes in stator 3 loss coefficient for both mechanisms is 7–10% of what is already a low value for stator 3 mid-span loss. In order to get a better perspective on the impact of the changes in stator 3 performance, we have related the changes in stator 3 loss to changes in stage 3 efficiency which are also include in Table 2 for comparison. The potential impact of indexing on stage 3 efficiency was calculated by assuming that stator 3 could be re-designed such that changes to stator 3 loss due to indexing were eliminated. This inherently assumes that rotor 3 performance does not change. The resultant estimated change in stage 3 efficiency at the peak pressure and peak efficiency conditions is 0.6% and 0.4%, respectively.

The results obtained in the present work indicate that indexing has only a small impact on the performance of the four-stage test compressor. It is reasonable to ask what the impact might be on a core compressor consisting of more stages. The present results can be used to estimate this impact as follows. Since the wakes from stators 1 and 2 are detectable at stator 3, we can assume that the change in loss of stator 3 is impacted by stators 1 and 2. Stator 2 loss is affected by stator 1 wakes, and perhaps shows less effect due to indexing than does stator 3 loss. We might also assume that stator 4 experiences at least as much change in loss due to indexing as does stator 3. However , if the stator 1 wake does not persist past rotor 4, the stator 4 loss change would equal that of stator 3. Making these simplified assumptions and using the stator 3 loss change of 0.6% measured at mid-span, we assume index-driven efficiency changes for stages 1,2,3, and 4 of 0.0, 0.3, 0.6, and 0.6% respectively. The calculated impact of these changes on the overall efficiency is a change of 0.4%. This is close to the measured overall change of 0.2%, considering that our simplified assessment has ignored any influence of indexing on rotor performance. Based upon the above it seems reasonable to postulate the following: 1) for stators that have low losses and thus moderate wake strength, such as those at the peak efficiency point, the impact of indexing is small; 2) as blades become more highly loaded with greater losses and larger wakes, the impact of indexing might be significant enough to warrant consideration during design; 3) the efficiency changes in a machine with a large number of stages might plateau after the first few stages since stator wakes can only persist through a few stages.

Table 2 Summary of Performance Changes (per stage basis) Due to Stator Indexing.

	Peak Pressure			Peak Efficiency		
	$\frac{\Delta\Psi_{avg}}{\Psi_{mean}}$	$\frac{\Delta\bar{\omega}}{\bar{\omega}_{mean}}$	$\Delta\eta_{isen}$	$\frac{\Delta\Psi_{avg}}{\Psi_{mean}}$	$\frac{\Delta\bar{\omega}}{\bar{\omega}_{mean}}$	$\Delta\eta_{isen}$
Overall	0.29%	-	0.2%	0.24%	-	0.2%
Stator 3	-	10%	-	-	5%	-
Stage 3	-	-	0.6%	-	-	0.4%
Passage-to-Passage differences						
Stator 3	-	7%	-	-	4%	-
Stage 3	-	-	0.4%	-	-	0.2%

Wake Interactions

During the course of establishing the stator wake indexing configurations it was discovered that certain indexing configurations resulted in stator wakes appearing to be almost entirely mixing out at the entrance to the downstream stator row. This effect is illustrated in Figures 8 and 9 which show mid-span stator wake profiles measured at two axial locations: just downstream of stator 2, and just upstream of stator 3. The results demonstrate how the measured wake profiles of stators 1 and 2 combine to form the circumferential distributions of total pressure measured at the stator 2 exit and stator 3 inlet stations for two different indexing configurations. In Figure 8 the wakes of stator 1 are aligned to impact the leading edge of stator 2. In Figure 9 the wakes of stator 1 are unaligned with the stator 2 leading edge such that they pass through the mid-passage of stator 2. Since our pitchwise surveys are accomplished by moving the stators relative to the probes, it was possible to perform pitchwise surveys of total pressure for four different cases: 1) with stator 2 fixed and only stator 1 moving, 2) with stator 1 fixed and only stator 2 moving, 3) with stator 1 and 2 aligned such that the wakes of stator 1 impact the leading edge of stator 2 while collectively moving both stators, and 4) with stators 1 and 2 unaligned such that the wakes of stator 1 pass through the mid-passage of stator 2 while collectively moving both stators. As shown in Figure 8a, the wake profile of case 3 contains remnants of the structure of the wake profiles of cases 1 and 2 above (i.e., stator-stator

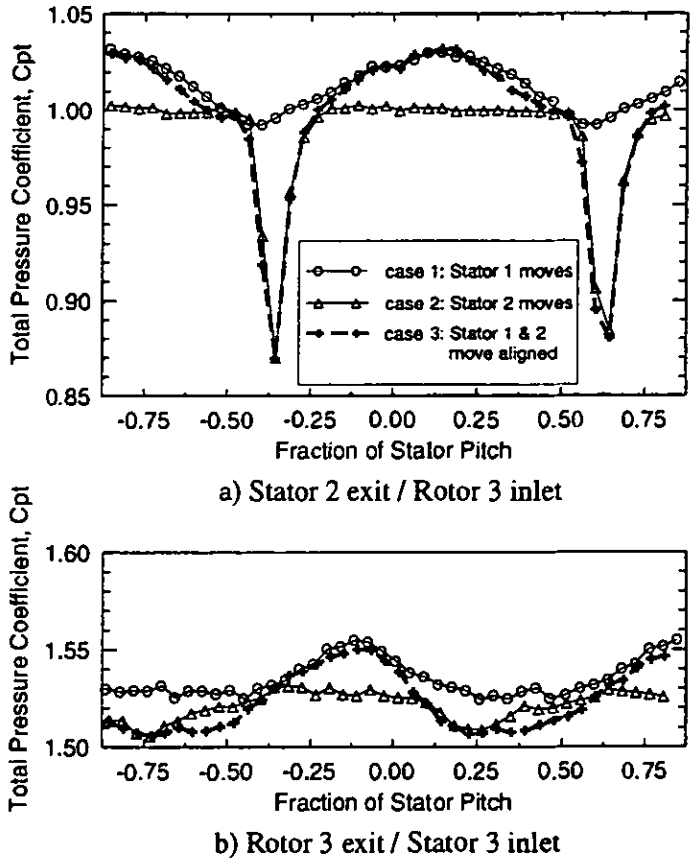

Figure 8 Mid-span stator wake profiles for peak efficiency condition at two different axial locations for the case when stators 1 and 2 are aligned.

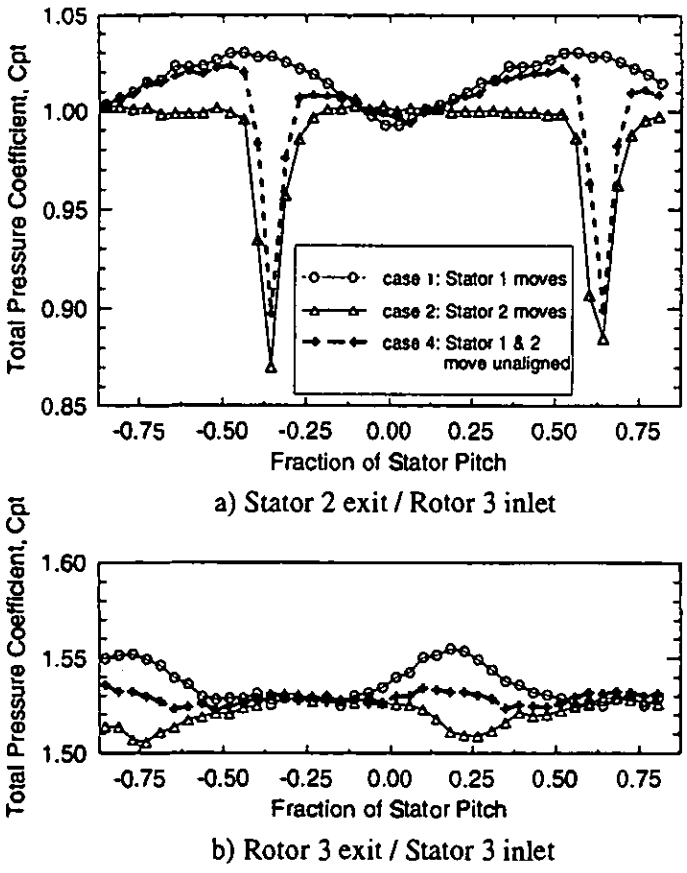

Figure 9 Mid-span stator wake profiles for peak efficiency condition at two different axial locations for the case when stators 1 and 2 are unaligned.

wake interactions). Stator-stator wake interactions are also evident in Figure 9a for the wake profiles obtained just downstream of stator 2 where the stator 1 wake acts to modulate the freestream region outside of the stator 2 wakes.

As shown in Figure 9b, the wakes of stator 2 appear to be almost completely mixed out for the case when stators 1 and 2 are unaligned and collectively moved past the probe, case 4. It's clear from Figures 8 and 9 that although the wakes of stator 1 and 2 are initially of different magnitudes at the stator 2 exit, they are of similar magnitude by the time they reach the station just upstream of stator 3 (Figures 8b and 9b). Thus, stator-stator wake interactions which are dependent on the relative positions of stators 1 and 2) is what makes the stator 2 wakes seem to mix out or disappear just upstream of stator 3 when stators 1 and 2 are unaligned, case 4 (Figure 9b). As would be expected, stator-stator wake interactions were also found to occur between stators 2 and 3 when surveyed ahead of stator 4, but to a lesser degree since the wakes of stators 2 and 3 were not of similar magnitude at that location. For stages with unequal blade counts the wake interactions will produce circumferential flow variations in the downstream blade rows which are not at the pitch of the downstream stator row. It may be necessary, therefore, to survey across more than one blade row pitch for accurate blade element performance measurements.

CONCLUSIONS

The results of this investigation quantify the impact of stator indexing on the LSAC overall and stator 3 blade row performance. For this investigation the following conclusions are drawn:

- The impact of stator indexing produced a 0.2 % change in overall efficiency at both peak pressure and peak efficiency conditions, and a 5 and 10% change in stator 3 total pressure loss coefficient, respectively.
- The impact of stator indexing on compressor performance was found to be small, and on the order of that due to manufacturing and assembly tolerances for the test compressor. However, as blades become more highly loaded the significance of these effects can be expected to increase.
- The stator indexing configuration corresponding to maximum performance is dependent on operating condition.

In addition, effects of stator-stator wake interactions are clearly shown and indicate that, for unequal blade row counts, it may be necessary to survey across more than one blade row pitch for accurate blade row performance measurements. Finally, it can be concluded that since most multistage compressors have a different number of stator blades in each stage, with the exception of some aft stage sets, the potential for performance gains due to stator indexing is expected to be even less than that measured in the present effort.

ACKNOWLEDGMENTS

The authors would like to thank Bill Darby, Rick Senyitko, and Charles Wasserbauer for their support of the experiments, and are especially grateful to Dr. Anthony Strazisar and Mr. Jerry Wood for their helpful suggestions and assistance throughout this research program.

REFERENCES

Arndt, N., "Blade Row Interaction in a Multistage Low-Pressure Turbine," ASME Paper A92-15678, 1991.

Engel, K., Eulitz, F., and Gebing, H., "Numerical Investigation of the Clocking Effects in a Multistage Turbine," AD-Vol. 49, Computational Fluid Dynamics in Aeropropulsion, ASME, 1995.

Griffin, Lisa W., Huber, Frank W., and Sharma, O.P., "Performance Improvement Through Indexing of Turbine Airfoils Part 2 - Numerical Simulation," ASME Paper No. 95-GT-28, 1995.

Huber, F.W., Johnson, P.D., Sharma, O.P., Staubach, J.B., and Gaddis, S.W., "Performance Improvement Through Indexing of Turbine Airfoils Part 1 - Experimental Investigation," ASME Paper No. 95-GT-27, 1995.

Schmidt, D.P., and Okiishi, T.H., "Detailed Measurements of the Periodically Unsteady Flow Produced by Rotor and Stator Wake Interaction in a Multi-stage Turbomachine," AIAA Paper No. A77-19894, 1977.

Schlicting, H., 1979, Boundary-Layer Theory, McGraw-Hill book Company, Inc., New York, N. Y.

Walker, Gregory J., "Effect of Wake-Wake Interactions on the Generation of Noise in Axial-Flow Turbomachinery," Proceedings of the 1st International Symposium on Air Breathing Engines, Paper No. A73-14129, 1972.

Walker, G.J., and Oliver, A.R., "The Effect of Interaction Between Wakes From Blade Rows in an Axial Flow Compressor on the Noise

Generated by Blade Interaction," Transactions of the ASME Journal of Engineering for Power," Paper No. 72-GT-15, 1972.

Wasserbauer, C.A., Weaver, H.F., and Senyitko, R.G., "NASA Low-Speed Axial Compressor for Fundamental Research," NASA TM 4635, 1995.

Wellborn, S. R., "Effects of Shrouded Stator Cavity Flows on Multistage Axial Compressor Aerodynamic Performance," NASA CR-198536, October, 1996. Wisler, D. C., "Core Compressor Exit Stage Study: Volume 1 - Blading Design," NASA CR-135391, December, 1977.